

Relative Permeabilities From Displacement Experiments With Full Account for Capillary Pressure

H.M. Helset,* SPE, Stavanger College; J.E. Nordvedt, SPE, RF-Rogaland Research; S.M. Skjæveland, SPE, Stavanger College; and G.A. Virnovsky, SPE, RF-Rogaland Research

Summary

Relative permeabilities are important characteristics of multiphase flow in porous media. Displacement experiments for relative permeabilities are frequently interpreted by the Johnson–Bossler–Naumann method neglecting capillary pressure. The experiments are therefore conducted at high flooding rates, which tend to be much higher than those experienced during reservoir exploitation. Another disadvantage is that the relative permeabilities only can be determined for the usually small saturation interval outside the shock. We present a method to interpret displacement experiments with the capillary pressure included, using in-situ measurements of saturations and phase pressures. The experiments can then be run at low flow rates, and relative permeabilities can be determined for all saturations. The method is demonstrated by using simulated input data.

Introduction

Relative permeabilities are important characteristics of multiphase flow in porous media. These quantities arise from a generalization of Darcy's law, originally defined for single-phase flow.¹ Relative permeabilities are used as input to simulation studies for predicting the performance of potential strategies for hydrocarbon-reservoir exploitation.

The relative permeabilities are usually determined from flow experiments performed on core samples. The most direct way to measure the relative permeabilities is by the steady-state method.¹ Each experimental run gives only one point on the relative permeability curve (relative permeability vs. saturation). To make a reasonable determination of the whole curve, the experiment has to be repeated at different flow-rate fractions. To cover the saturation plane in a three-phase system, a large number of experiments have to be performed. The method is therefore very time-consuming.

Relative permeabilities can also be calculated from a displacement experiment. Typically, the core is initially saturated with a single-phase fluid. This phase is then displaced by injecting the other phases into the core. For the two-phase case, Welge² showed how to calculate the ratio of the relative permeabilities from a displacement experiment. Efros³ was the first to calculate individual relative permeabilities from displacement experiments. Later, Johnson *et al.*⁴ presented the calculation procedure in a more rigorous manner, and the method is often referred to as the Johnson–Bossler–Naumann (JBN) method. The analysis has also been extended to three phases.⁵ In this approach, relative permeabilities are calculated at the outlet end of the core; saturations vs. time at the outlet end is determined from the cumulative volumes produced and time derivatives of the cumulative volumes produced, and relative permeabilities vs. time are calculated from measurements of pressure drop over the core and the time derivative of the pressure drop.

Although the JBN method is frequently used for relative permeability determination, it has several drawbacks. The method is based on the Buckley–Leverett theory of multiphase flow in porous media.⁶ The main assumption in this theory is that capillary pressure can be neglected. In homogenous cores, capillary effects

are most important at the outlet end of the core and over the saturation shock front. To suppress capillary effects, the experiments are performed at a high flow rate. Usually, these rates are significantly higher than those experienced in the underground reservoirs during exploitation. Another major disadvantage is that relative permeabilities only can be calculated for the spreading part of the saturation profile, because the theory is not valid in the vicinity of the saturation shock where capillary effects are significant. In a water/oil system, the saturation-shock interval is frequently more than 50% of the total mobile-saturation range. This means that relative permeabilities cannot be determined for a substantial range of saturation. Extrapolating the estimated relative permeability curves into the saturation interval corresponding to the saturation shock can be very difficult.

A better alternative is to reduce the flow rate in the experiments, and include capillary pressure in the analysis. In this work, we use the fact that a reduced flow rate will lead to a spreading of the shock front. The front will translate with a fixed shape (denoted as a traveling wave or a stabilized capillary zone¹). We propose a new method to calculate relative permeabilities for the traveling-wave part of the profile. We consider a displacement experiment performed at a sufficiently low rate such that the shock front is spread out into a traveling wave. By this method, relative permeabilities can be calculated for a substantially larger saturation range than is possible with the standard JBN method. Calculation of relative permeabilities from the stabilized capillary zone has also been performed previously, but using only an approximate analysis.⁷ Note that this approach can be applied for both two-phase and three-phase relative-permeability estimation.

In this approach, we will use only in-situ measurements of saturations and phase pressures. In recent years, techniques have been developed for in-situ measurement of saturations of the fluids in the core, which has a potential to enhance our understanding of the flow in the porous medium. In-situ saturation measurements can be performed by various techniques: X-ray attenuation,⁸ X-ray computer tomography,⁹ gamma emission,⁷ ultrasound,¹⁰ microwaves,¹¹ and nuclear magnetic resonance.¹² In addition, in-situ pressure measurements have been performed by several experimenters.^{7,10,11} One expects that, through use of thin water-wet and oil-wet membranes, the individual phase pressures can be measured.

This paper is organized as follows: First, the theory for the traveling wave solution for three-phase flow with gravity is developed to allow calculation of relative permeabilities from measurements of saturation and phase pressures. A method based on solutions of a linear least-squares problem, including regularization, is used to avoid differentiation of measured quantities. This leads to a more stable solution. The new interpretation method is demonstrated on artificially generated data from simulation of a two-phase displacement experiment. Pointwise and integral calculations are compared, and noise is added.

Methodology

In a displacement experiment, the phases are injected at fixed rate fractions into a core initially saturated with one or all phases. According to the Buckley–Leverett theory, the saturation profile will, in general, consist of a shock and a spreading part. When capillary effects are important, the shock will be spread out, and is called a traveling wave. A traveling wave solution has the

* Now with RF-Rogaland Research

form^{1,13,14}

$$S(x, t) = S(\xi), \quad \xi = x - vt. \quad \dots \dots \dots (1)$$

Substituting $\xi = x - vt$ into the conservation equation,

$$\frac{\partial u_i}{\partial x} + \phi \frac{\partial S_i}{\partial t} = 0, \quad i = 1, 2, 3, \quad \dots \dots \dots (2)$$

and integrating gives

$$u_i = C_i^* + \phi v S_i = u(C_i + v_D S_i), \quad \dots \dots \dots (3)$$

where C_i^* is a constant of integration, $C_i = C_i^*/u$, $u = \sum_i u_i$, and $v_D = \phi v/u$. Inserting Eq. 3 into Darcy's law,

$$u_i = -\frac{kk_{r_i}}{\mu_i} \left(\frac{\partial p_i}{\partial x} - \rho_i g_x \right), \quad i = 1, 2, 3, \quad \dots \dots \dots (4)$$

we obtain the pressure gradient along the traveling wave part of the saturation profile,

$$\frac{\partial p_i}{\partial x} = -\frac{\mu_i u}{k_{r_i} k} (C_i + v_D S_i) + \rho_i g_x, \quad i = 1, 2, 3. \quad \dots \dots \dots (5)$$

Note that the expression for the pressure gradient only involves the relative permeability of one phase. The constant C_i can be determined from $C_i = f_i^+ - v_D S_i^+$, where

$$f_i = \frac{\lambda_i}{\lambda_i} \left(1 + \frac{k}{u} g_x \sum_{j \neq i} \lambda_j \Delta \rho_{ij} \right), \quad \dots \dots \dots (6)$$

where $\lambda_i = k_{r_i}/\mu_i$, $\lambda_i = \sum_i \lambda_i$, and $\Delta \rho_{ij} = \rho_i - \rho_j$. The velocity v of the traveling wave is the same as the velocity of the shock,^{1,14}

$$v = \frac{u f_i^+ - f_i^-}{\phi S_i^+ - S_i^-}. \quad \dots \dots \dots (7)$$

Here, $+$ and $-$ denote the states to the right and left of the traveling wave, respectively. The velocity of the traveling wave can also be measured directly by monitoring the saturation profile at two different positions along the core.

Away from the traveling-wave part of the profile, we can assume that the gradient of the capillary pressure can be neglected. The pressure gradient for this part is then the same for all phases,

$$\frac{\partial p_i}{\partial x} = -\frac{u}{k\lambda_i} + g_x \frac{\sum_i \lambda_i \rho_i}{\lambda_i}, \quad i = 1, 2, 3. \quad \dots \dots \dots (8)$$

The pressure gradient at the traveling wave part of the saturation profile, Eq. 5, must necessarily follow the traveling wave. Using

$$\frac{\partial p_i}{\partial x}(x, t) = \frac{\partial p_i}{\partial x}(x - vt), \quad \dots \dots \dots (9)$$

we get (see Appendix)

$$\frac{\partial p_i}{\partial t} = \frac{\mu_i v u}{k_{r_i} k} \left(C_i + \frac{\phi v}{u} S_i \right) - v \rho_i g_x + v \frac{\partial p_i}{\partial x}(S_i^+) \dots \dots \dots (10)$$

for each Phase i , where

$$\frac{\partial p_i}{\partial x}(S_i^+) = \text{const} \dots \dots \dots (11)$$

is the pressure gradient in Phase i at the constant initial saturation S_i^+ . The constants C_i are related by $\sum_i C_i = 1 - v_D$. When $\partial p_i/\partial t$ is known, the relative permeability of Phase i can be determined explicitly, independent of the pressures in the other phases.

Note that if Phase i is absent initially, we have $f_i^+ = 0$, $S_i^+ = 0$, and hence, $C_i = 0$. The dimensionless velocity $v_D = v\phi/u$ is then given by the saturation S_i^- and the fractional flow f_i^- at the left side of the traveling wave. In general, the saturation profile will

consist of a combination of a traveling wave and a spreading wave. In a two-phase system having a typical S-shaped fractional flow curve, the traveling wave will have higher velocity than the spreading part of the saturation profile. The expressions in Eq. 10 are then still valid because they only involve quantities ahead of the traveling wave. This is also true for a three-phase system.¹⁵

Integral Equation. The relative permeabilities may be determined from Eq. 10 by differentiation of $p_i(t)$. However, the numerical differentiation process will magnify errors, and oscillatory solutions may result. We can reformulate Eq. 10 as an integral equation, considering Phase 1 here:

$$\int_0^t \frac{\partial p_1}{\partial t'} dt' = p_1(t) - p_1(0), \quad \dots \dots \dots (12)$$

where $p_1(t)$ is the pressure in Phase 1 as a function of time measured at a point x , and $p_1(0)$ is the pressure at the start of the traveling wave profile. Inserting from Eq. 10 and neglecting gravity for simplicity in the notation only, we get

$$\int_0^t \frac{1}{k_{r_1}(t')} [C_1 + v_D S_1(t')] dt' = \tilde{p}_1(t), \quad \dots \dots \dots (13)$$

$$\text{where } \tilde{p}_1(t) = \left[p_1(t) - p_1(0) - vt \frac{\partial p_1}{\partial x}(S_1^+) \right] \frac{k}{v u \mu_1}. \quad \dots \dots (14)$$

Eq. 13 is a Volterra integral equation of the first kind¹⁶ and represents a class of inverse problems.

The unknown function, $h(t) = 1/k_{r_1}(t)$, is expanded by B-splines,

$$h(t) = \sum_{j=1}^{n_h} c_j^h B_{n,j}^m(\tilde{y}_h, t). \quad \dots \dots \dots (15)$$

The saturation, $S_1(t)$, will be measured directly. However, to deal with measurement errors in discrete measurements, we use B-splines expansion also here:

$$S_1(t) = \sum_{k=1}^{n_s} c_k^s B_{s,k}^m(\tilde{y}_s, t). \quad \dots \dots \dots (16)$$

Inserting Eq. 15 into Eq. 13 we get

$$\tilde{p}_1(t_i) = \sum_{j=1}^{n_h} c_j^h \left\{ C_1 \int_0^{t_i} B_{n,j}^m(\tilde{y}_h, t') dt' + v_D \int_0^{t_i} B_{n,j}^m(\tilde{y}_h, t') S_1(t') dt' \right\}, \quad \dots \dots \dots (17)$$

where $S_1(t)$ is given by Eq. 16. This equation has the linear form $A\tilde{x} = \tilde{b}$, where the unknowns x_j are the coefficients c_j^h . Both the integral of a B-spline and the inner product of two B-splines can be calculated exactly,¹⁷ and hence, A can be determined analytically. The vector \tilde{b} is found through Eq. 14.

To determine $h(t)$, and subsequently, the relative permeabilities, we solve the linear least-squares problem

$$\min_{\tilde{x}} \|A\tilde{x} - \tilde{b}\|^2, \quad \dots \dots \dots (18)$$

subject to linear inequality constraints

$$G\tilde{x} \leq \tilde{x}^c. \quad \dots \dots \dots (19)$$

These linear inequality constraints ensure that $h(t)$ is positive and monotonic; see Watson *et al.*¹⁸ for details of the structure of G and \tilde{x}^c .

It is also possible to write the integral equation with saturation

as the independent variable,

$$\int_{S^+}^S \frac{1}{\lambda_1(S')} [C_1 + v_D S'] \frac{dt}{dS'} dS' = \tilde{p}_1(S). \quad \dots\dots\dots (20)$$

Here, we shall determine the function, $1/k_{r1}(S)$, which we may assume is a positive, decreasing, and convex function. The convexity criterion would probably have rendered sufficient smoothness, and additional regularization would not have been required. However, this equation involves the determination of dS/dt , and differentiation of measurement data usually introduces relatively large uncertainties. We will therefore proceed with Eq. 13 using time as the independent variable.

Tikhonov Regularization. To obtain a suitably smooth solution of the problem in Eq. 17, we amend the linear least-squares problem by using Tikhonov regularization.¹⁹ The Tikhonov regularized solution \tilde{x}_Λ is defined as the solution of the least-squares problem,

$$\min_{\tilde{x}} \{ \|\mathbf{A}\tilde{x} - \tilde{b}\|^2 + \Lambda \|\mathbf{L}\tilde{x}\|^2 \}. \quad \dots\dots\dots (21)$$

Here, Λ is the weight given to the minimization of the seminorm $\|\mathbf{L}\tilde{x}\|$ of the solution relative to minimization of the residual norm $\|\mathbf{A}\tilde{x} - \tilde{b}\|$. We will use the second derivative as the regularization operator L . This means that we expect $1/k_{ri}$ vs. time to be relatively smooth functions.

It is important to choose a proper value for the regularization parameter Λ . A variety of methods have been proposed. Hansen²⁰ recommends the L-curve method where Λ is chosen from a plot of $\|\mathbf{A}\tilde{x} - \tilde{b}\|$ vs. $\|\mathbf{L}\tilde{x}\|$. Yang and Watson²¹ choose the largest value of Λ that does not compromise the fit between simulated and measured data.

Length of the Traveling Wave Profile. It is important to estimate the length of the stabilized zone; the profile must be wide enough so that measurements can be made, but the length should be small compared with the length of the core. For the traveling-wave part of the saturation profile we have, following Marle,¹

$$\frac{\partial S_1}{\partial x} = \frac{u}{k} \frac{\lambda_1 + \lambda_2}{\lambda_1 \lambda_2} \frac{1}{dp_c/dS_1} [C_1 + v_D S_1], \quad \dots\dots\dots (22)$$

where we again have neglected gravity for simplicity. By integrating Eq. 22, we get

$$X_D = \frac{k}{ul\mu_2} I, \quad \dots\dots\dots (23)$$

where X_D is the length of the traveling wave normalized with the length l of the core, and I is the integral,

$$I = \int_{S_1^-}^{S_1^+} \frac{k_{r2}(\partial p_c/\partial S_1)}{(C_1 + v_D S_1)(1 + (k_{r2}\mu_1/k_{r1}\mu_2)) - 1} dS_1. \quad \dots\dots\dots (24)$$

This is the same expression as given by Jones-Parra and Calhoun²² if we use

$$\frac{\partial f_1}{\partial S_1} = v_D \quad \dots\dots\dots (25)$$

in the stabilized zone. The integration is taken over the whole saturation range of the traveling wave. However, the integrand is singular at the limits S_1^+ and S_1^- . The integration should, therefore, be performed over a slightly smaller saturation interval to avoid problems with the calculations.

To calculate the integral I and estimate the length of the traveling wave before the relative permeabilities are estimated, a model of capillary pressure and relative permeabilities is needed. Brooks and Corey presented a model that connects drainage-capillary pressure and relative permeability to pore-size distribution through a single parameter λ .²³ Theoretically, λ may have any value greater than

zero, being large for media with relatively uniform pore sizes and small for media with wide pore-size variation. The commonly encountered range for λ is between 2 and 4 for various sandstones. The capillary pressure/saturation relation is

$$S_1^* = \left(\frac{p_b}{p_c} \right)^\lambda, \quad \text{for } p_c \geq p_b, \quad \dots\dots\dots (26)$$

where p_b is the threshold pressure, and $S_1^* = (S_1 - S_{1r})/(1 - S_{1r})$ is the mobile wetting phase saturation. Relative permeabilities are given by

$$k_{r1} = (S_1^*)^{(2+3\lambda)/\lambda} \quad \dots\dots\dots (27)$$

$$\text{and } k_{r2} = (1 - S_1^*)^2 [1 - (S_1^*)^{(2+\lambda)/\lambda}]. \quad \dots\dots\dots (28)$$

Using this model, the integral I in Eq. 24 can be calculated for different values of λ . We assume a drainage process where the initial saturation is $S_1^* = 1.0$. Fig. 1 shows I/p_b as functions of λ for three different viscosity ratios μ_2/μ_1 . The integration is taken from $(S_1^- + 0.01)$ to $(S_1^+ - 0.01)$ to avoid singularities. The value of I/p_b decreases with increasing λ , and with decreasing viscosity ratio. The parameters λ and p_b are found from measurements of capillary pressure. The value of the integral I is then found from Fig. 1. Using this in Eq. 23, the length of the profile can be calculated. Note that the capillary pressure and relative permeability models in Eqs. 26 through 28 are not always sufficient to represent real data. In such cases, other representations must be used (splines, polynomials, etc.).

If the saturation profile consists of both a spreading part and a traveling wave part, the saturation S_1^- in Eq. 23 will not be exactly the "shock front saturation," but rather, the saturation at which the spreading part and the traveling wave part are connected.²⁴

The expression in Eq. 23 has also been used by Potter and Lyle²⁵ to estimate the length of the stabilized zone. They only used qualitative estimates and did not explicitly calculate the length of the zone.

Description of Example

To determine the relative permeability of Phase i from Eq. 13, we need to measure the saturation and pressure of the phase as a function of time at one position along the core. Only data for the traveling wave profile can, of course, be interpreted by Eq. 13.

We also need to determine v_D and C_1 in Eq. 13. If the saturation profile only consists of a traveling wave, the velocity is determined from the initial and boundary conditions by Eq. 7. In general, the saturation profile will consist of a spreading wave and a traveling wave. From in-situ measurements of saturation (or pressure) at two positions along the core, the traveling-wave part of the saturation profile can be identified, and its velocity can be determined. This will be necessary in most cases, because we rarely will know if the saturation profile only is a traveling wave, or if there is a spreading part in addition.

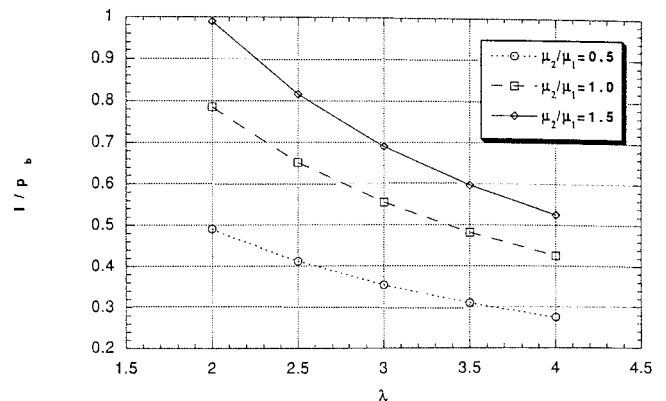


Fig. 1—The integral I in Eq. 24 divided by p_b as a function of λ for different viscosity ratios μ_2/μ_1 .

The constant $C_1 = f_1^+ - v_D S_1^+$ is determined from the initial saturation in the core and the corresponding relative permeability. If the core is fully saturated with Phase 1, we have $C_1 = 1 - v_D$, and $C_1 = 0$ if the core is saturated with Phase 2. If the core initially contains both fluids, the relative permeability can be determined from the steady-state value at this saturation.

If the traveling-wave saturation profile is distorted by the end effect, the measurements will be erroneous. The end effect must therefore be minimized. If the core is much longer than the spread of the traveling wave, measurements can be taken in the middle of the core.

As an example, synthetic data from a numerical simulator were used as input to the analysis. We performed a one-dimensional simulation of a horizontal coreflood where a water/oil mixture displaces oil. The fractional flow of water at the inlet is $f_1^- = 0.79$, and is chosen such that the saturation profile consists of only a traveling wave. In the simulation, 400 uniform gridblocks were used. The data $S_1(t)$, $p_1(t)$, and $p_2(t)$ were taken from Block 100 at 12.5 cm from the core inlet. The parameters used in the simulation study are given in **Table 1**. The relative permeabilities are Corey-type exponential functions of saturation. The capillary-pressure curve is linear from $P_c(S_1 = 1.0) = 0$ to $P_c(0.22) = 6$ kPa, but it is much steeper for lower saturations.

Results

The simulated data $S_1(t)$ taken from Block 100 and Block 300 are shown in **Fig. 2**. The time scale for the data from Block 300 is shifted with the time delay $\Delta t = \Delta x/v$ between the measurements, Δx is the distance between the measurement positions, and v is the velocity of the front. The match between the curves is very good, validating that the profile indeed is a traveling wave. For each of the saturation- and pressure-data series, 660 data points were used. In the following, we demonstrate the calculation of the relative permeabilities both by the pointwise and the integral-equation method. We consider artificial data both with and without experimental errors added. In cases with errors, we have used normally distributed errors with zero mean and a standard deviation representative of experimental uncertainties.

Pointwise Method. The relative permeability can be calculated directly from Eq. 10. This involves differentiation, and errors are magnified. One way of improving the situation is through smoothing of experimental data. **Fig. 3** shows the resulting relative permeabilities when taking the derivative between successive pressure data without smoothing. In this case, we use noise-free data; only the numerical errors from the calculations are present. Also shown are the results from a coarse-grid (100 blocks) simulation. Whereas the results from the fine-grid simulations are relatively smooth, just the numerical errors present in the coarse-grid simulations result in significant oscillations. The oscillations are largest in the oil-relative permeability at low water saturation. The oil pressure is approximately constant, and the calculation of k_{r2} is very sensitive to errors because $dp_2/dt \approx 0$ in the denominator. Using real experimental data will result in even more oscillations.

Length of the core	50 cm
Cross-section area	11.1 cm ²
k_h, k_v	100 md
ϕ	0.20
μ_1, μ_2	1.0, 1.2 cp
Residual saturations (S_1, S_2)	0.16, 0.0
S_1^+	0.16
f_1^-	0.79
Total flow rate	0.2 cm ³ /min
No. of grid blocks	400

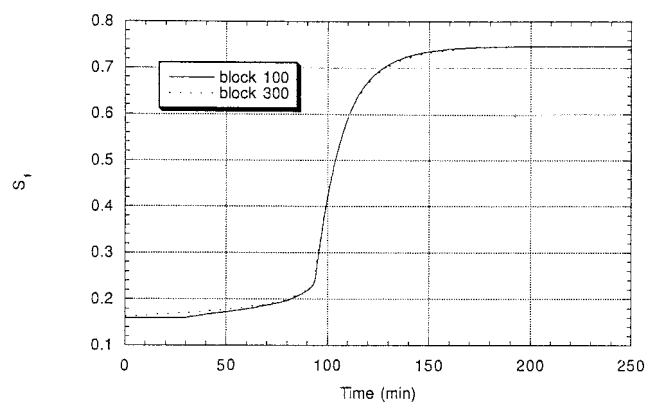


Fig. 2—Water saturation vs. time from simulation, taken from Blocks 100 and 300. To match the curves, the time scale for data from Block 300 is shifted with the time delay $\Delta t = \Delta x/v$ between the measurements.

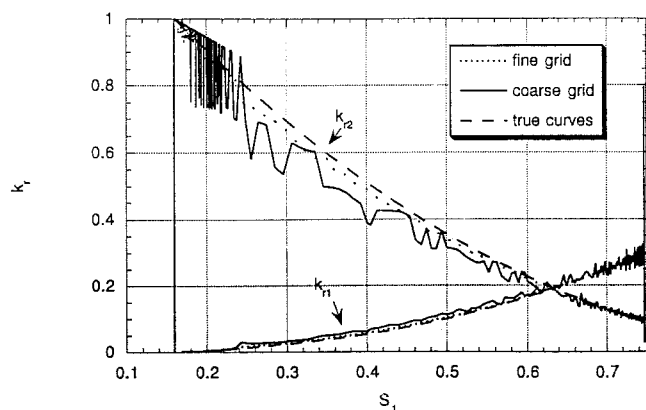


Fig. 3—Relative permeabilities for Phase 1 and Phase 2 from pointwise calculation. Fine grid is 400 blocks, whereas coarse grid is 100 blocks.

Integral Method. To avoid differentiation of measured data, we calculate the relative permeability from Eq. 13. We represent the measured saturations by a B-spline expansion and determine the coefficients through the solution of a linear least-squares problem. This enables a good approximation of the saturation measurements, even with measurement errors present. The B-spline expansion is also convenient when performing the calculations for solving the linear system in Eq. 17 with respect to the coefficients c_j^h .

First, we show the result without any errors in the saturation or pressure measurements. To have sufficient flexibility, 50 knots are used in the partition of the time interval. No regularization is used in this case. The resulting relative permeability curves for both phases are shown in **Fig. 4**, together with the true relative-permeability curves. For the relative permeability of Phase 1 (water), there is good match between the calculated and true curves, whereas there is a small deviation between the calculated and true curves for the oil-relative permeability. The deviation is caused by numerical dispersion. The curves here are smoother than the results from the pointwise method shown in **Fig. 3**.

Next, errors are added to the data. Errors in saturations are smoothed out well when the measurements of saturation vs. time are approximated by a B-spline function. We will not discuss this further here, but rather concentrate on the effect that errors in pressure have on the solution.

To the pressure data $p_1(t)$ are added normally distributed errors with zero mean and variance equal to 1% of the maximum pressure. This corresponds to the accuracy in the pressure measurements. No errors are added to the saturation data. We use 50 knots in the representation of $h(t)$. We have found that using too few knots leads to problems in solving the integral equation. The solution of the integral equation gives the inverse of the relative permeability

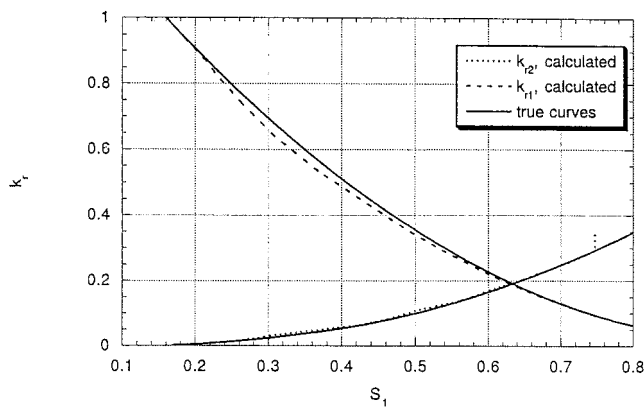


Fig. 4—Relative permeability curves for Phase 1 and Phase 2 calculated by the integral method. No errors are added to the data. The true relative permeability curves are shown for comparison.

as a function of time. The results are shown in **Fig. 5** for two different values of Λ . The corresponding plot of relative permeability vs. saturation is shown in **Fig. 6**. The value $\Lambda = 1.0$ is close to the corner of the L-curve, and should be a good choice according to Hansen.²⁰ However, oscillations are still present in the estimated curve, because of the extra flexibility given from the added errors. High Λ -values have given solutions which, on average, deviate from the true solution; see Kolltveit *et al.*²⁶ Here, we have not investigated further the effect of using a high Λ -value for different realization of the error vector.

Discussion

A new method to calculate relative permeabilities from the traveling-wave part of the saturation profile has been presented. In-situ measurements of saturations and phase pressures are needed. Capillary pressure is included in the analysis, and the experiments can be run at low rates. The new method makes it possible to calculate relative permeabilities for the saturation interval that cannot be analyzed by the standard JBN method (i.e., the saturation shock).

To make good measurements of saturation and phase pressure over the traveling-wave part of the saturation profile, the traveling wave must be sufficiently spread out. This is accomplished by lowering the injection rate. The response time of the pressure transducers must also be analyzed together with the velocity and the spread of the profile. The response must be sufficiently fast to allow measurements of phase pressures at transient conditions.

The spread of the profile can be estimated from Eq. 23 or from simulation. In either case, an initial guess of relative permeabilities and capillary pressure is needed, giving only a rough estimate of the true saturation profile. The spread of the traveling wave should, however, not be so wide that the measurements are affected by the

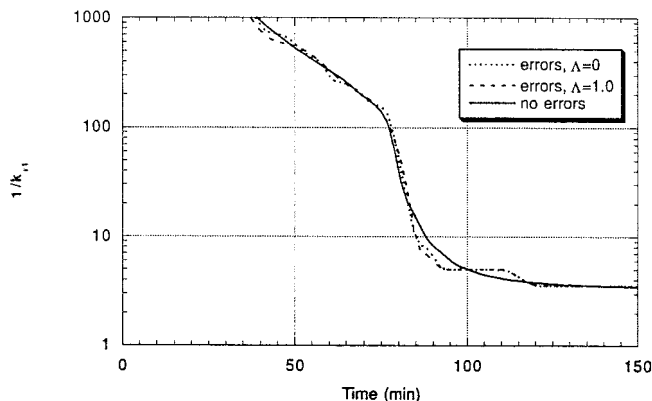


Fig. 5—Inverse of the water-relative permeability vs. time from estimation.

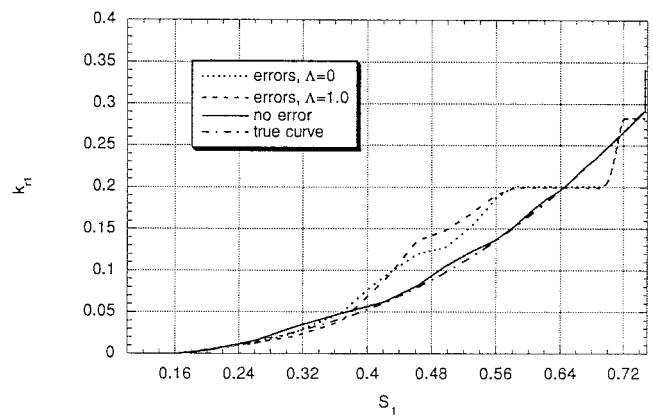


Fig. 6—Water-relative permeability vs. water saturation from estimation compared to the true water-relative permeability curve. Results with and without experimental errors added, and using different regularization parameter Λ are shown.

end effect. The whole traveling wave must pass the measurement position before it is influenced by the end effect. A long core can be used to ensure that the end effect is important in only a small fraction of the core length. The end effect is discussed further by Helset *et al.*²⁷

Eq. 10, which allows calculation of relative permeabilities, involves the time derivative of the measured-phase pressure. Taking derivatives of measured quantities will magnify measurement errors. We present an integral method to deal with errors in the measurement in a systematic way. Expanding the inverse of the relative permeability by B-spline functions reduces the problem to a system of linear equations that is solved by a least-squares procedure. Tikhonov regularization is used to ensure smooth solutions. The choice of the regularization parameter Λ is important. Wrong choice of Λ will either lead to oversmoothing or under-smoothing of the solution. Objective methods for choosing the regularization parameter have been proposed. However, different criteria might give different values for Λ , and care should be taken to choose the proper Λ . We have used the L-curve method here because it uses directly the balance between minimizing the set of linear equations and the regularization term.

In general, the saturation profile will consist of a combination of a traveling wave and a spreading wave. In a two-phase system having a typical S-shaped fractional-flow curve, the traveling wave will have higher velocity than the spreading part of the saturation profile. The expressions in Eq. 10 are then still valid because they only involve quantities ahead of the traveling wave. This is also true within each wave family in a three-phase system.¹⁵

Conclusions

A method for calculating relative permeabilities from the traveling wave part of the saturation profile in a displacement experiment has been derived. In the analysis, capillary pressures are included. From this analysis, relative permeabilities from displacement experiments can be determined for the whole saturation range, in contrast to the traditional JBN method, which is not valid over the saturation shock. Using the new method, it is also possible to perform the experiments at low flow rates corresponding to realistic reservoir rates. The experimental data needed are in-situ measurements of saturation and phase pressure. The equations for determining the relative permeabilities for each phase are decoupled, meaning that the determination of relative permeability of one phase only depends upon the saturation and pressure of this phase.

Nomenclature

- A = matrix, t, s
- \vec{b} = vector, t, s
- B = B-spline function, dimensionless
- C = constant of integration, dimensionless
- f = fractional flow, dimensionless

- g = scalar component of gravity, L/t^2 , m/s^2
- $h(t) = 1/k_{ri}(t)$
- I = Integral defined in Eq. 24, m/Lt^2 , Pa
- k = permeability, L^2 , m^2
- l = length of the core, L, m
- L = operator
- n = number of B-spline, dimensionless
- p = pressure, m/Lt^2 , Pa
- S = saturation, dimensionless
- t = time, t, s
- u = Darcy velocity, L/t, m/s
- v = velocity of traveling wave, L/t, m/s
- $v_D = v\phi/u$, dimensionless
- x = spatial coordinate, L, m
- \vec{x} = vector, dimensionless
- X = length of traveling wave, L, m
- \vec{y} = partition vector, dimensionless
- λ = mobility, L^3t/m , $m^2/Pa \cdot s$
- Λ = regularization parameter, dimensionless
- μ = fluid viscosity, m/Lt , $Pa \cdot s$
- $\xi = x - vt$, traveling-wave coordinate, L, m
- ρ = fluid density, m/L^3 , kg/m^3
- ϕ = porosity

Subscripts

- b = threshold pressure
- c = capillary
- D = dimensionless
- h = horizontal
- i = fluid phase; $i = 1, 2$
- r = relative, residual
- t = total
- v = vertical

Superscripts

- $+$ = right state of a shock
- $-$ = left state of a shock
- m = order of spline

Operators

- ' = derivative
- Δ = difference, $\Delta\rho_{ij} = \rho_i - \rho_j$
- $\|\cdot\|$ = 2-norm

Acknowledgment

We thank The Research Council of Norway for a doctorate scholarship for Hans Martin Helset.

References

1. Marle, C.M.: "Multiphase Flow in Porous Media," Editions Technip, Paris (1981).
2. Welge, H.: "A Simplified Method for Computing Oil Recovery by Gas or Water Drive," *Trans.*, AIME (1952) **195**, 91.
3. Efros, D.A.: "Determination of Relative Permeabilities and Distribution Functions at Water-Oil Displacement," [in Russian] *Doklady Akad Nauk*, (1956) **110**, 5, 746.
4. Johnson, E.F., Bossler, D.P., and Naumann, V.O.: "Calculation of Relative Permeability from Displacement Experiments," *Trans.*, AIME, (1959) **216**, 370.
5. Virnovsky, G.A.: "Determination of Relative Permeabilities in a Three-Phase Flow in a Porous Medium," *Izvestiya Akademii Nauk SSSR*, [in Russian], *Mekhanika Zhidkosti i Gaza*, (1984), 5, English translation: *Fluid Dynamics*, Plenum Publishing Corp. (1985).
6. Buckley, S.E. and Leverett, M.C.: "Mechanism of Fluid Displacement in Sands," *Trans.*, AIME, (1942) **146**, 107.
7. Kolltveit, K. *et al.*: "Using Explicit and Implicit Methods to Calculate Relative Permeabilities from *In Situ* Measurements," paper presented at the 1990 First Society of Core Analysts European Core Analysis Symposium, London, 21–23 May.
8. Oak, M.J., Baker, L.E. and Thomas, D.C.: "Three-Phase Relative Permeability of Berea Sandstone," *JPT* (August 1990) 1054.

9. Hove, A., Ringen, J.K., Read, P.A.: "Visualization of Laboratory Corefloods With the Aid of Computerized Tomography of X-Rays," *SPE* (May 1987) 148; *Trans.*, AIME, **283**.
10. Kalaydjian, F.J.-M.: "Dynamic Capillary Pressure Curve for Water/Oil Displacement in Porous Media: Theory vs. Experiment," paper SPE 24813 presented at the 1992 SPE Annual Technical Conference and Exhibition, Washington, DC, 4–7 October.
11. Honarpour, M.M., Huang, D.D. and Dogru, A.H.: "Simultaneous Measurements of Relative Permeability, Capillary Pressure, and Electrical Resistivity with Microwave System for Saturation Monitoring," paper SPE 30540 presented at the 1995 SPE Annual Technical Conference and Exhibition, Dallas, 22–25 October.
12. Chen, S. *et al.*: "NMR Imaging of Multiphase Flow in Porous Media," *AIChE Journal*, (1993), **39**, No. 6, 1473.
13. Smoller, J.: *Shock Waves and Reaction-Diffusion Equations* (Second ed.), Springer Verlag, New York (1994).
14. Virnovsky, G.A., Helset, H.M., and Skjæveland, S.M.: "Stability of Displacement Fronts in WAG Operations," paper SPE 28622 presented at the 1994 SPE Annual Technical Conference and Exhibition, New Orleans, 25–28 September.
15. Helset, H.M.: "Three-Phase Flow and Capillarity in Porous Media," PhD dissertation, The U. of Bergen, Norway (1996).
16. Linz, P.: *Analytical and Numerical Methods for Volterra Equations*, SIAM, Philadelphia (1985).
17. Schumaker, L.L.: *Spline Functions: Basic Theory*, J. Wiley and Sons, New York (1981).
18. Watson, A.T. *et al.*: "A Regression-Based Method for Estimating Relative Permeabilities from Displacement Experiments," *SPE* (August 1988) 953.
19. Tikhonov, A.N. and Arsenin, V.Y.: *Solutions of Ill-Posed Problems*, Wiley, New York (1977).
20. Hansen, P.C.: "Analysis of Discrete Ill-Posed Problems by means of the L-curve," *SIAM Review*, (December 1992), **34**, No. 4, 561.
21. Yang, P. and Watson, A.T.: "A Bayesian Methodology for Estimating Relative Permeability Curves," *SPE* (May 1991) 259.
22. Jones-Parra, J. and Calhoun, Jr., J.C.: "Computation of a Linear Flood by the Stabilized Zone Method," *Trans.*, AIME, (1953) **198**, 335.
23. Honarpour, M.M., Koederitz, L., Harvey, A.H.: *Relative Permeability of Petroleum Reservoirs*, (1994).
24. Le Fur, B.: "Influence de la capillarite et de la gravite sur le deplacement non miscible unidimensionnel dans un milieu poreux," *Journal de mecanique*, (Juin 1962), **1**, No. 2, 213.
25. Potter, G. and Lyle, G.: "Measuring Unsteady-State Gas Displacing Liquid Relative Permeability of High Permeability Samples," paper SCA-9419 presented at the 1994 Society of Core Analysts International Symposium, Stavanger, Norway, 12–14 September.
26. Kolltveit, K. *et al.*: "Estimation of Capillary Pressure Functions From Centrifuge Data," *Proc.*, International Conference on Inverse Problems in Engineering: Theory and Practice, Le Croisic, France (June 1996).
27. Helset, H.M., Skjæveland, S.M., and Virnovsky, G.A.: "Application of Composite Membranes to Determine Relative Permeabilities from Displacement Experiments," paper presented at the 1996 Society of Core Analysts International Symposium, Montpellier, France, 8–10 September.

Appendix: Derivation of the Time Derivative of the Phase Pressure (Eq. 10)

For the pressure gradient of Phase i at the traveling-wave part of the saturation profile, we have

$$\frac{\partial p_i}{\partial x}(x, t) = \frac{\partial p_i}{\partial x}(x - vt) \dots \dots \dots (A-1)$$

We can write

$$\begin{aligned} \frac{\partial}{\partial x} \left(\frac{\partial p_i}{\partial x}(x, t) \right) &= -\frac{1}{v} \frac{\partial}{\partial t} \left(\frac{\partial p_i}{\partial x}(x, t) \right) \\ &= -\frac{1}{v} \frac{\partial}{\partial x} \left(\frac{\partial p_i}{\partial t}(x, t) \right) \dots \dots \dots (A-2) \end{aligned}$$

or

$$\frac{\partial}{\partial x} \left[\frac{\partial p_i}{\partial x} (x, t) + \frac{1}{v} \frac{\partial p_i}{\partial t} (x, t) \right] = 0. \quad \dots\dots\dots (A-3)$$

This implies

$$\frac{\partial p_i}{\partial x} (x, t) + \frac{1}{v} \frac{\partial p_i}{\partial t} (x, t) = A, \quad \dots\dots\dots (A-4)$$

where A is not dependent of x . At the core outlet, $x = L$; $S_i = S_i^+$, the phase pressure, being a function of saturation, is constant before breakthrough of the traveling wave. This implies $\partial p_i / \partial t (L, t) = 0$, and, from Eq. A-4,

$$A = \frac{\partial p_i}{\partial x} (L, t) = \frac{\partial p_i}{\partial x} (S_i^+). \quad \dots\dots\dots (A-5)$$

Using Eqs. A-5 and 5 in Eq. A-4 gives Eq. 10. Note that Eq. 10 is only valid before breakthrough. Modified equations valid after breakthrough are given by Helset *et al.*²⁷

SI Metric Conversion Factors

cp × 1.0*	E-03 = Pa · s
ft × 3.048*	E-01 = m
in. × 2.54*	E+00 = cm
knot × 5.144 444	E-01 = m/s
md × 9.869 233	E-04 = μm ²
psi × 6.894 757	E+00 = kPa

*Conversion factor is exact.

SPEREE



Helset



Nordtvedt



Skjæveland



Virnovsky

Hans M. Helset is a research scientist with RF-Rogaland Research, Stavanger, Norway. His research interests are in physics of multiphase flow in porous media and reservoir engineering. Helset holds an MS degree in physics from the Norwegian Inst. of Technology and a PhD degree in physics from Bergen U., Norway. **Jan-Erik Nordtvedt** is research manager for reservoir technology and improved oil recovery at RF-Rogaland Research in Bergen, Norway. His research interests include two- and three-phase flow through porous media, parameter estimation, and inverse problems. He holds MS and PhD degrees in physics from the U. of Bergen. Nordtvedt is a Technical Editor for *SPE Reservoir Evaluation & Engineering*. **Svein M. Skjæveland** is a professor of reservoir engineering at Stavanger College. He holds PhD degrees in physics from the Norwegian Inst. of Technology and in petroleum engineering from Texas A&M U. **George A. Virnovsky** is a chief scientist in the IOR/Reservoir Technology Group at RF-Rogaland Research in Stavanger. His interests are in modeling of multiphase flow in porous media and reservoir simulation. He holds an MS degree in electrical engineering from Gubkin Petroleum Academy and a PhD degree in reservoir engineering from VNIlneft in Moscow, Russia.